# Transportation Marketplace Rate Forecast Using Signature Transform

Haotian Gu \* Xin Guo  $^{\dagger \ddagger}$  Timothy L. Jacobs  $^{\ddagger}$  Philip Kaminsky  $^{\ddagger}$  Xinyu Li  $^{\dagger}$  February 15, 2024

#### Abstract

Freight transportation marketplace rates are typically challenging to forecast accurately. In this work, we have developed a novel statistical technique based on signature transforms and have built a predictive and adaptive model to forecast these marketplace rates. Our technique is based on two key elements of the signature transform: one being its universal nonlinearity property, which linearizes the feature space and hence translates the forecasting problem into linear regression, and the other being the signature kernel, which allows for comparing computationally efficiently similarities between time series data. Combined, it allows for efficient feature generation and precise identification of seasonality and regime switching in the forecasting process.

An algorithm based on our technique has been deployed by Amazon trucking operations, with far superior forecast accuracy and better interpretability versus commercially available industry models, even during the COVID-19 pandemic and the Ukraine conflict. Furthermore, our technique is able to capture the influence of business cycles and the heterogeneity of the marketplace, improving prediction accuracy by more than fivefold, with an estimated annualized saving of \$50MM.

# 1 Introduction

Overview. Linehaul freight transportation costs make up a significant portion of overall Amazon transportation costs. To manage these costs, Amazon has developed a variety of tools to manage linehaul capacity mix and procurement. One key input to all of these models is a forecast of transportation freight marketplace rates, which however are notoriously difficult to forecast – they are driven by a number of factors: the ever-changing network of tens of thousands of drivers, shippers of all sizes with a mix of occasional, seasonal, and regular demand, a huge set of brokers, traditional and digital exchanges, and local, regional, national, and international economic factors of all kinds. In addition, the transportation marketplace frequently goes through fundamental shifts – either because of wars, pandemics, fuel prices, or due to shifting international trade patterns.

Although Amazon has purchased externally created forecasts for some time, these forecasts are neither explainable nor sufficiently accurate to meet specific Amazon needs. To address this challenge, we have built a forecasting model based on time series data to predict weekly freight marketplace rates for the North America market, at both the national and the regional levels. Our approach incorporates an innovative signature-based statistical technique capable of efficiently capturing significant fluctuations in transportation marketplace rates.

<sup>\*</sup>Department of Mathematics, University of California, Berkeley, Berkeley, CA 94720, USA **Email:** haotian\_gu@berkeley.edu

<sup>&</sup>lt;sup>†</sup>Department of Industrial Engineering & Operations Research, University of California, Berkeley, CA 94720, USA **Email:** {xinguo, xinyu\_li}@berkeley.edu

<sup>&</sup>lt;sup>‡</sup>Middle Mile Marketplace Science, Amazon Research, USA **Email:** {xnguo, timojaco, philipka}@amazon.com

The key challenges in time series forecasting. Time series data consists of sequential observations recorded over time and is ubiquitous: finance, economics, transportation, weather, and energy prices. Given time series data, forecasting additional data points is critical for informed decision-making and process optimization in almost every organization and industry.

Time series prediction models such as Autoregressive Integrated Moving Average (ARIMA) [26] and Exponential Smoothing [13] assume that the time series are stationary, which is not the case for freight marketplace rates. Moreover, ARIMA has limited ability to capture seasonality and long-term trends [20], and Exponential Smoothing may be insufficient for abrupt changes or outliers and produce unstable forecasts [29]. Furthermore, these methods rely solely on historical data from the time series, which is inadequate in capturing the causal relation between the economic factors and the marketplace rates. Meanwhile, machine learning algorithms such as Long Short-Term Memory Neural Networks [33] and Gated Recurrent Units [10], though capable of capturing nonlinear relationship and complex patterns in time series data, will require substantially more training data which is not available in our case.

Indeed, one of the main challenges in analyzing time series data is their ever-changing statistical properties, due to factors including changes in business and economic cycles, shifts in policy, or changes in market conditions. In our case, the market itself has recently experienced shifts in *regimes* and *seasonality* [16], in terms of volatility, trends, and cyclical patterns, partly due to the COVID-19 pandemic and the Ukraine conflict.

Machine learning models and signature transform. Much of statistical learning theory relies on finding a feature map that embeds the data (for instance, samples of time series) into a high-dimensional feature space. Two requirements for an ideal feature map are universality, meaning that non-linear functions of the data are approximated by linear functionals in the feature space; and characteristicness, meaning that the expected value of the feature map characterizes the law of the random variable. It is shown that with the technique of the signature transform these two properties are in duality and therefore often equivalent [27]. This is the primary inspiration for our proposed signature-based forecasting technique for our forecast models.

Originally introduced and studied in algebraic topology [5, 6], the *signature transform*, sometimes referred to as the *path signature* or simply *signature*, has been further developed in rough path theory [24, 12], introduced for financial applications [23, 1, 22, 17] and machine learning [32, 31, 21, 4, 18], and most recently to time series data analysis [25, 9, 11]. Given any continuous or discrete time series, their signature transform produces a vector of real-valued features that extract information such as order and area, and explicitly considers combinations of different channels. The signature of time series uniquely determines the time series, and does so in a computationally efficient way. Most importantly, every continuous function of a time series data may be asymptotically approximated by a linear functional of its signature. In other words, signature transform linearizes the otherwise complicated feature space, and thus is a powerful tool for feature generation and pattern identification in machine learning.

Our work. We propose a novel signature-based statistical technique for the time series forecasting problem. This is based on two key elements of the signature transform. The first is the universal nonlinearity property of the signature transform, which linearizes the feature space of the time series data and hence translates the forecasting problem into a linear regression analysis. The second is the signature kernel which allows for computationally efficient comparison of similarities between time series data. Technically, this is to identify different "signature feature maps", the statistical counterpart of identifying different distributions for a given time series data, albeit in the linearized features space from the signature transform.

Our approach starts by collecting data including a hundred of market supply and demand factors, and runs a correlation test between the marketplace rate and the factors to remove non-significant factors and to identify factors that may be colinear. We then exploit the universal nonlinearity property of

signature transform to construct signature features as suitable candidates for the "internal" features. To avoid issues of overfitting and co-linearity between the signature feature and the external factors, and to improve the forecast accuracy, we adopt the two-step LASSO for the regression analysis [2]. Finally, this two-step LASSO is enhanced with adaptive weight using a signature kernel, which enables capturing changes in regimes or seasonality. Combined, this leads to our signature-based adaptive two-step LASSO approach. This novel signature-transform-based technique for data analysis allows for efficient feature generation and more precise identification of seasonality and regime switching embedded in the data.

Implementation and real-time performance. This signature-based adaptive two-step LASSO algorithm has been implemented for the trucking operations in Amazon since November 2022. Performance analysis shows that our forecast model presents superior performance than commercially available forecast models, while providing significantly better interpretability. Despite the onset of COVID-19 and the Ukraine conflict, it captures the influence of business cycles and heterogeneity of the market-place, improves prediction accuracy by more than fivefold, and has an estimated annualized saving of approximately \$50MM.

# 2 Technical Background

# 2.1 Signatures of Continuous Paths

We begin with the definition of signatures of continuous piecewise smooth paths.

**Notation** Let  $\mathbb{R}^{d_1} \otimes \mathbb{R}^{d_2} \otimes \cdots \otimes \mathbb{R}^{d_n}$  denote the space of all real tensors with shape  $d_1 \times d_2 \times \cdots \times d_n$ . Define a binary operation called *tensor product*, denoted by  $\otimes$ , which maps a tensor of shape  $(d_1, \ldots, d_n)$  and a tensor of shape  $(e_1, \ldots, e_m)$  to a tensor of shape  $(d_1, \ldots, d_n, e_1, \ldots, e_m)$  via  $(A_{i_1, \ldots, i_n}, B_{j_1, \ldots, j_m}) \mapsto A_{i_1, \ldots, i_n} B_{j_1, \ldots, j_m}$ . When applied to two vectors, it reduces to the outer product. Let  $(\mathbb{R}^d)^{\otimes k} = \mathbb{R}^d \otimes \cdots \otimes \mathbb{R}^d$ , and  $v^{\otimes k} = v \otimes \cdots \otimes v$  for  $v \in \mathbb{R}^d$ , in each case with k-1 many  $\otimes$ .

**Definition 1.** Let  $a < b \in \mathbb{R}$ , and  $X = (X^1, \dots, X^d) : [a, b] \to \mathbb{R}^d$  be a continuous piecewise smooth path. The signature of X is then defined as the collection of iterated integrals

$$\operatorname{Sig}(X) = \left( \int_{a < t_1 < \dots < t_k < b} dX_{t_1} \otimes \dots \otimes dX_{t_k} \right)_{k \ge 0}$$

$$= \left( \left( \int_{a < t_1 < \dots < t_k < b} dX_{t_1}^{i_1} \cdots dX_{t_k}^{i_k} \right)_{1 \le i_1, \dots, i_k \le d} \right)_{k > 0}, \tag{1}$$

where  $\otimes$  denotes the tensor product,  $dX_t = \frac{dX_t}{dt} dt$ , and the k = 0 term is taken to be  $1 \in \mathbb{R}$ . The truncated signature of depth N of X is defined as

$$\operatorname{Sig}^{N}(X) = \left( \int_{a < t_{1} < \dots < t_{k} < b} dX_{t_{1}} \otimes \dots \otimes dX_{t_{k}} \right)_{0 \le k \le N}.$$
 (2)

**Remark 1.** The signature can be defined more generally on paths of bounded variation [11], but the above definition suffices for our purposes.

**Example 1.** Suppose  $X:[a,b] \to \mathbb{R}^d$  is the linear interpolation of two points  $x,y \in \mathbb{R}^d$ , so that  $X_t = x + \frac{t-a}{b-a}(y-x)$ . Then its signature is the collection of tensor products of its total increment:

$$Sig(X) = \left(1, y - x, \frac{1}{2}(y - x)^{\otimes 2}, \frac{1}{6}(y - x)^{\otimes 3}, \dots, \frac{1}{k!}(y - x)^{\otimes k}, \dots\right),\tag{3}$$

which is independent of a, b.

**Example 2.** Suppose  $X : [a,b] \to \mathbb{R}$  is a one-dimensional smooth path. Then its signature is the collection of powers of its total increment:

$$\operatorname{Sig}(X) = \left(1, X(b) - X(a), \frac{1}{2} (X(b) - X(a))^{2}, \frac{1}{6} (X(b) - X(a))^{3}, \dots, \frac{1}{k!} (X(b) - X(a))^{k}, \dots\right), \tag{4}$$

which is independent of  $X(t), t \in (a, b)$ . Furthermore, when X(t) is a random process, the expected signature

$$\mathbb{E}\left[\operatorname{Sig}(X)\right] = \left(1, \mathbb{E}\left[X(b) - X(a)\right], \frac{1}{2}\mathbb{E}\left[\left(X(b) - X(a)\right)^{2}\right], \dots, \frac{1}{k!}\mathbb{E}\left[\left(X(b) - X(a)\right)^{k}\right], \dots\right),$$
(5)

whenever it exists, describes precisely the moments of X(b) - X(a). Thus, for a high-dimensional stochastic process X(t), the expected signature naturally forms the generalization of the moments of the process. In other words, for a stochastic process X(t), its expected signature characterizes the law of X(t) up to tree-like equivalence, as proved in [8].

Example 2 shows that the signature for a one-dimensional path only depends on its total increment. In general, it implies that the signature of a path itself may not carry sufficient information to fully characterize the path. Nevertheless, this problem may be resolved by considering the *time-augmented* version of the original path (see Definition 4, Theorem 1 and 2 below).

## 2.2 Signature of Discrete Data

To define and compute signatures of discrete data streams, one can simply do linear interpolations and then apply signature transforms.

**Definition 2.** The space of streams of data is defined as

$$\mathcal{S}\left(\mathbb{R}^d\right) = \left\{ oldsymbol{x} = (oldsymbol{x}_1, \dots, oldsymbol{x}_n) : oldsymbol{x}_i \in \mathbb{R}^d, n \in \mathbb{N} 
ight\}.$$

Given  $\mathbf{x} = (\mathbf{x}_1, \dots, \mathbf{x}_n) \in \mathcal{S}(\mathbb{R}^d)$ , the integer n is called the length of  $\mathbf{x}$ . Furthermore for  $a, b \in \mathbb{R}$  such that a < b, fix

$$a = u_1 < u_2 < \dots < u_{n-1} < u_n = b.$$
 (6)

Let  $X = (X^1, ..., X^d)$ :  $[a,b] \to \mathbb{R}^d$  be continuous such that  $X_{u_i} = \boldsymbol{x}_i$  for all i, and linear on the intervals in between. Then X is called a linear interpolation of  $\boldsymbol{x}$ .

**Definition 3.** Let  $\mathbf{x} = (\mathbf{x}_1, \dots, \mathbf{x}_n) \in \mathcal{S}(\mathbb{R}^d)$  be a stream of data. Let X be a linear interpolation of  $\mathbf{x}$ . Then the signature of  $\mathbf{x}$  is defined as  $\operatorname{Sig}(\mathbf{x}) = \operatorname{Sig}(X)$ , and the truncated signature of depth N of  $\mathbf{x}$  is defined as  $\operatorname{Sig}^N(\mathbf{x}) = \operatorname{Sig}^N(X)$ .

**Definition 4.** Given a path  $X:[a,b] \to \mathbb{R}^d$ , define the corresponding time-augmented path by  $\widehat{X}_t = (t,X_t)$ , a path in  $\mathbb{R}^{d+1}$ .

#### 2.3 Key Properties of Signature

**Theorem 1** (Uniqueness [15]). Let  $X : [a,b] \to \mathbb{R}^d$  be a continuous piecewise smooth path. Then  $\operatorname{Sig}(\widehat{X})$  uniquely determines X up to translation.

In fact, the signature not only determines a path uniquely up to translation, but also *linearizes* any continuous functions of the path, as stated in the next theorem.

**Theorem 2** (Universal nonlinearity [1]). Let F be a real-valued continuous function on continuous piecewise smooth paths in  $\mathbb{R}^d$  and let  $\mathcal{K}$  be a compact set of such paths. Furthermore assume that  $X_0 = 0$  for all  $X \in \mathcal{K}$ . (To remove the translation invariance.) Let  $\varepsilon > 0$ . Then there exists a linear functional L such that for all  $X \in \mathcal{K}$ ,  $|F(X) - L(\operatorname{Sig}(\widehat{X}))| < \varepsilon$ .

This universal nonlinearity is the key property of the signature transform and is important for our model, and in general for applications in feature augmentations. See [23], [21], [25] for examples.

Note that the signature by definition is an infinite-dimensional tensor. In practice, one can only compute the truncated signature  $\operatorname{Sig}^N$  in Equation (2) up to some depth N. The next result guarantees that reminder terms in the truncation decay factorially.

**Theorem 3** (Factorial decay [24]). Let  $X : [a,b] \to \mathbb{R}^d$  be a continuous piecewise smooth path. Then

$$\left\| \int_{a < t_1 < \dots < t_k < b} dX_{t_1} \otimes \dots \otimes dX_{t_k} \right\| \le \frac{C(X)^k}{k!}$$

where C(X) is a constant depending on X and  $\|\cdot\|$  is any tensor norm on  $(\mathbb{R}^d)^{\otimes k}$ .

The next property about signatures, Theorem 4, is the invariance to time reparameterisations. It implies that the signature encodes the data by its arrival order and independently of its arrival time. This is a desired property in many applications such as hand-writing recognition [32], [31]. Meanwhile, there is an interesting interplay between Theorem 2 and Theorem 4: in a problem where time parameterisations are irrelevant, it suffices to compute the signature of X by Theorem 4; However, if time parameterisation is important, then according to Theorem 2, applying the signature transform to the time-augmented path  $\widehat{X}$  ensures that parameterisation-dependent features are still learned.

**Theorem 4** (Invariance to time reparameterisations [24]). Let  $X : [0,1] \to \mathbb{R}^d$  be a continuous piecewise smooth path. Let  $\psi : [0,1] \to [0,1]$  be continuously differentiable, increasing, and surjective. Then  $\operatorname{Sig}(X) = \operatorname{Sig}(X \circ \psi)$ .

Note that by Theorem 4, the signature of a stream of data is independent of the choice of  $u_i$  in a linear interpolation in Equation (6). Meanwhile, by Theorem 2, in order to learn parameterisation-dependent features, one can apply the signature transform to the time-augmented data stream  $\hat{\boldsymbol{x}} = (\hat{\boldsymbol{x}}_1, \dots, \hat{\boldsymbol{x}}_n)$ , where  $\hat{\boldsymbol{x}}_i = (\boldsymbol{x}_i, t_i) \in \mathbb{R}^{d+1}$ , and  $t_i$  is the time when the data point  $\boldsymbol{x}_i$  arrives.

Let  $\boldsymbol{x} = (\boldsymbol{x}_1, \dots, \boldsymbol{x}_n) \in \mathcal{S}\left(\mathbb{R}^d\right)$  be a data stream of length n in  $\mathbb{R}^d$ . Then  $\operatorname{Sig}^N(\boldsymbol{x})$  has

$$M(d,N) := \sum_{k=0}^{N} d^k = \frac{d^{N+1} - 1}{d-1}$$
 (7)

components. In particular, the number of components does not depend on the length of the data stream n. The truncated signature maps the infinite-dimensional space of streams of data  $\mathcal{S}\left(\mathbb{R}^d\right)$  into a finite-dimensional space of dimension  $\left(d^{N+1}-1\right)/(d-1)$ . Thus the signature is an efficient way to tackle long streams of data, or streams of variable length.

#### 2.4 Computation of Signature Transform

The signature transform of a data stream can be computed in an efficient and tractable way, with the help of Chen's identity [24, 4]. It starts by introducing the following  $\boxtimes$  operation:

With  $A_0 = B_0 = 1$ , define  $\otimes$  by

$$\boxtimes : \left(\prod_{k=1}^{N} \left(\mathbb{R}^{d}\right)^{\otimes k}\right) \times \left(\prod_{k=1}^{N} \left(\mathbb{R}^{d}\right)^{\otimes k}\right) \to \prod_{k=1}^{N} \left(\mathbb{R}^{d}\right)^{\otimes k},$$

$$(A_{1}, \dots A_{N}) \boxtimes (B_{1}, \dots, B_{N}) \mapsto \left(\sum_{j=0}^{k} A_{j} \otimes B_{k-j}\right)_{1 \leq k \leq N}.$$
(8)

Chen's identity [12] states that the image of the signature transform forms a group structure with respect to  $\boxtimes$ . That is, given a sequence of data  $(x_1, \ldots, x_L) \in \mathcal{S}(\mathbb{R}^d)$  and some  $j \in \{2, \ldots, L-1\}$ ,

$$\operatorname{Sig}^{N}((x_{1},\ldots,x_{L})) = \operatorname{Sig}^{N}((x_{1},\ldots,x_{j})) \boxtimes \operatorname{Sig}^{N}((x_{j},\ldots,x_{L})).$$

Furthermore, from Example 1, the signature of a sequence of length two can be computed explicitly from the definition. Letting

$$\exp: \mathbb{R}^d \to \prod_{k=1}^N \left( \mathbb{R}^d \right)^{\otimes k}, \quad \exp: v \to \left( v, \frac{v^{\otimes 2}}{2!}, \frac{v^{\otimes 3}}{3!}, \dots, \frac{v^{\otimes N}}{N!} \right), \tag{9}$$

then

$$\operatorname{Sig}^{N}((x_{1}, x_{2})) = \exp(x_{2} - x_{1}).$$

Chen's identity further implies that the signature transform can be computed by

$$\operatorname{Sig}^{N}((x_{1},\ldots,x_{L})) = \exp(x_{2}-x_{1}) \boxtimes \exp(x_{3}-x_{2}) \boxtimes \cdots \boxtimes \exp(x_{L}-x_{L-1}).$$

$$(10)$$

Equation (10) implies that computing the signature of an incoming stream of data is efficient and scalable. Indeed, suppose one has obtained a stream of data and computed its signature. Then after the arrival of some more data, in order to compute the signature of the entire signal, one only needs to compute the signature of the new piece of information, which is then computed via the tensor product with the previously-computed signature.

Improving computational efficiency. Recall from Equation (10) that the signature may be computed by evaluating several  $\boxtimes$  in Equation (8) and exp in Equation (9). We begin by noticing that the key component in the computation is to evaluate

$$\left(\prod_{k=1}^{N} \left(\mathbb{R}^{d}\right)^{\otimes k}\right) \times \mathbb{R}^{d} \to \prod_{k=1}^{N} \left(\mathbb{R}^{d}\right)^{\otimes k}, \quad A, z \mapsto A \boxtimes \exp(z).$$

Instead of computing  $A \boxtimes \exp(z)$  conventionally through the composition of exp and  $\boxtimes$ , [18] suggests to speed up the computation by Horner's method. More specifically, it is to expand

$$A \otimes \exp(z) = \left(\sum_{i=0}^{k} A_i \otimes \frac{z^{\otimes (k-i)}}{(k-i)!}\right)_{1 \leq k \leq N},$$

so that the k-th term can be computed by

$$\sum_{i=0}^{k} A_i \otimes \frac{z^{\otimes (k-i)}}{(k-i)!} = \left( \left( \cdots \left( \left( \frac{z}{k} + A_1 \right) \otimes \frac{z}{k-1} + A_2 \right) \otimes \frac{z}{k-2} + \cdots \right) \otimes \frac{z}{2} + A_{k-1} \right) \otimes z + A_k.$$

As proved in [18], this method has uniformly (over d, N) fewer scalar multiplications than the conventional approach, and reduces the asymptotic complexity of this operation from  $\mathcal{O}(Nd^N)$  to  $\mathcal{O}(d^N)$ . Furthermore, this rate is asymptotically optimal, since the size of the result (an element of  $\prod_{k=1}^{N} (\mathbb{R}^d)^{\otimes k}$ ), is itself of size  $\mathcal{O}(d^N)$ .

# 3 Forecasting Problem and Our Approach

# 3.1 Forecasting Problem

The freight marketplace rate forecast problem involves two time series  $\{x_{\tau}\}_{{\tau}\in\mathbb{N}^+}$  and  $\{y_{\tau}\}_{{\tau}\in\mathbb{N}^+}$ . Here,  $x_{\tau}\in\mathcal{X}\subseteq\mathbb{R}^{d_0}$  is a  $d_0$ -dimensional vector representing values of the key economic factors that drive the supply and demand in the freight marketplace at time  $\tau$ . Factors from the market supply side include information regarding the supply of drivers and trucks and fuel/oil prices, and some market demand factors are imports, agriculture information, manufacturing activities, housing indexes, and railway transport. Additionally,  $y_{\tau}\in\mathcal{Y}\subseteq\mathbb{R}$  is the freight marketplace rate at time  $\tau$ . Previously, Amazon relied on a commercial service to obtain forecasts for future freight marketplace rates. However, those forecasts lacked accuracy and transparency. To address these, we consider the following forecast problem.

The general goal of our forecast problem is to find models  $f_{\Delta t}^* \in \mathcal{F} \subseteq \{f | f : \mathcal{X} \to \mathcal{Y}\}$  such that  $f_{\Delta t}^*(\boldsymbol{x}_{\tau}) \approx y_{\tau+\Delta t}$ , for  $\Delta t = 1, 2, 3, \dots, \Delta T$ , where  $\Delta T \in \mathbb{N}^+$  denotes the longest forecast horizon and  $\mathcal{F}$  is the class of all admissible models. More precisely, given the data up to time  $t: \{(\boldsymbol{x}_{\tau}, y_{\tau})\}_{\tau=1,2,\dots,t}$ , in order to make prediction for  $y_{t+\Delta t}$ , one standard approach to find  $f_{\Delta t}^* \in \mathcal{F}$  is by solving the following optimization problem:

$$f_{\Delta t}^* \in \operatorname*{arg\,min}_{f \in \mathcal{F}} \left\{ \frac{1}{t - \Delta t} \sum_{\tau=1}^{t - \Delta t} L\left(f(\boldsymbol{x}_{\tau}), y_{\tau + \Delta t}\right) \right\},\tag{11}$$

where  $L: \mathcal{Y} \times \mathcal{Y} \to \mathbb{R}$  is a loss function measuring the difference between the model prediction  $f(\boldsymbol{x}_{\tau})$  and the actual  $y_{\tau+\Delta t}$ . Once  $f_{\Delta t}^*$  is obtained, the prediction of  $y_{t+\Delta t}$  is given by  $\hat{y}_{t+\Delta t} := f_{\Delta t}^*(\boldsymbol{x}_t)$ .

# 3.2 Our Approach

We will present a signature-based adaptive two-step LASSO approach that we have developed and implemented in Amazon, which has demonstrated excellent performance in solving this problem.

**Data.** Our approach and experiment start by collecting data involving over a hundred of national and regional market supply and demand factors, downloaded from the governmental public websites, including Federal Reserve Bank and Bureau of Labor Statistics, as well as industrial databases such as Logistic Manager. The time range for the data is from 2018 to 2022.

**External factor preprocessing.** We first run a correlation test between the marketplace rate and the factors to remove non-significant factors, with further correlation analysis to identify factors that may be colinear. After this round of elimination, over forty factors remain, including consumer price index, housing index, oil and gas drilling, logistic managers' index, employment information, weather, and other market benchmarks.

Internal features via signature transform. Besides the "external" factors  $\boldsymbol{x}_{\tau}$ , most time series forecasting approaches, such as ARIMA, also construct "internal" features from the history of  $y_{\tau}$ . Those "internal" features may help to characterize the trend, momentum, and stationarity of  $y_{\tau}$ . We, instead, exploit the universal nonlinearity property of signature transform (Theorem 2), and construct signature features as suitable candidates for the "internal" features.

More specifically, for any time step  $\tau \in \mathbb{N}^+$  and time window size  $l \in \mathbb{N}$ , denote  $y_{\tau-l:\tau} := (y_{\tau-l}, \dots, y_{\tau})$  as the slice of the time series  $\{y_t\}_{t\in\mathbb{N}^+}$  from time  $\tau-l$  to  $\tau$ . The feature vector for predicting  $y_{\tau+\Delta t}$  consists of both the economic factors  $\boldsymbol{x}_{\tau}$  and the depth-N signature features  $\operatorname{Sig}^N(y_{\tau-l:\tau})$ . We denote the concatenation of those two sets of features as  $[\boldsymbol{x}_{\tau}, \operatorname{Sig}^N(y_{\tau-l:\tau})]$ , whose dimension is denoted by d.

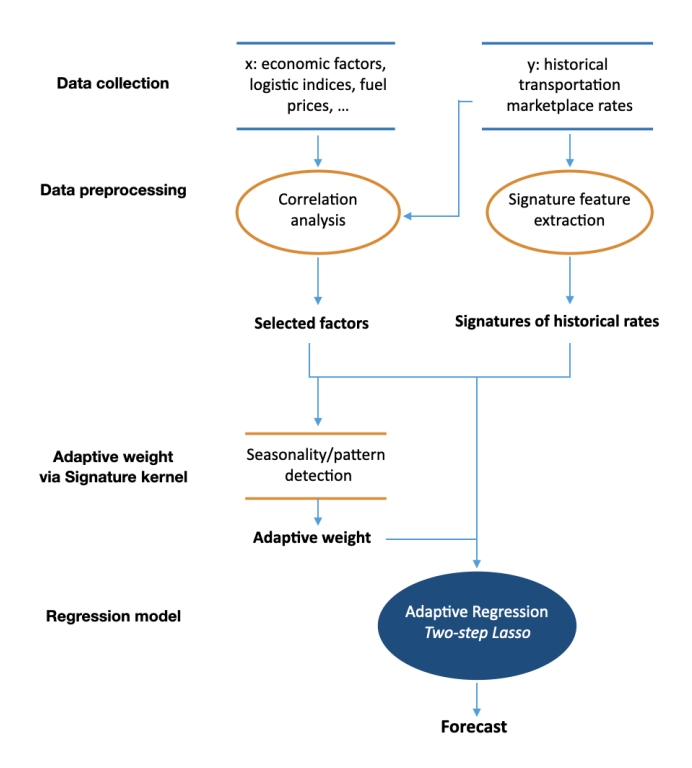


Figure 1: The Data Flow of the Adaptive Two-step LASSO via Signature Kernel (Algorithm 2)

**Two-step LASSO.** The universal nonlinearity property of the signature transform linearizes the feature space, hence translating the forecasting problem into a linear regression analysis. Since the dimension d of the feature vector may be relatively large compared to the number of historical samples, especially when the time step t is small, we adopt the approach of two-step LASSO to avoid overfitting and the issue of co-linearity especially between the signature feature and the external factors. The first step is to select the factors by solving the standard LASSO regression [30], [34], [35]. This is to add an  $L_1$ -regularization to model coefficients in the ordinary least square objective. This  $L_1$ -regularization will encourage the sparsity of model coefficients, and prevent the over-fitting problem. In the second step, an OLS with only the selected factors is applied. This two-step LASSO estimation procedure has been shown to produce a smaller bias than standard LASSO for a range of models [2], [7].

More precisely, recall that the LASSO regression is to solve the following optimization problem:

$$\widehat{\boldsymbol{\theta}}_{\text{LASSO},\Delta t}^{\lambda} \in \operatorname*{arg\,min}_{\boldsymbol{\theta} \in \mathbb{R}^d} \left\{ \frac{1}{t - \Delta t} \sum_{\tau=1}^{t - \Delta t} \left( y_{\tau + \Delta t} - \left[ \boldsymbol{x}_{\tau}, \operatorname{Sig}^N(y_{\tau - l:\tau}) \right] \cdot \boldsymbol{\theta} \right)^2 + \lambda \|\boldsymbol{\theta}\|_1 \right\}. \tag{12}$$

Here the constant  $\lambda$ , called the regularization parameter, controls the sparsity of coefficients: a higher value of  $\lambda$  leads to a smaller number of nonzero coefficients in  $\widehat{\boldsymbol{\theta}}_{\mathrm{LASSO},\Delta t}^{\lambda}$ . In the two-step LASSO, the first step is to select the factors by solving the LASSO regression in Equation (12), and get  $\widehat{\boldsymbol{\theta}}_{\mathrm{LASSO},\Delta t}^{\lambda}$ . In the second step, the subsequent OLS refitting is to find  $\overline{\boldsymbol{\theta}}_{\mathrm{LASSO},\Delta t}^{\lambda}$  such that

$$\overline{\boldsymbol{\theta}}_{\text{LASSO},\Delta t}^{\lambda} \in \underset{\text{supp}[\boldsymbol{\theta}] = \text{supp}[\widehat{\boldsymbol{\theta}}_{\text{LASSO},\Delta t}]}{\text{arg min}} \left\{ \frac{1}{t - \Delta t} \sum_{\tau=1}^{t - \Delta t} \left( y_{\tau + \Delta t} - \left[ \boldsymbol{x}_{\tau}, \text{Sig}^{N}(y_{\tau - l : \tau}) \right] \cdot \boldsymbol{\theta} \right)^{2} \right\}.$$
(13)

Adaptive weight via signature kernel. In the classical approach of two-step LASSO, each historical sample is given equal weight in the optimization problem to obtain the model at time t. However,

this equal-weight scheme may fail to account for changes of regime or seasonality. Instead, a more effective approach would be to dynamically assign weights based on their similarity to the current period. This is precisely what we propose, as elaborated below.

First, recall the signature feature map (Theorem 2),

$$\Phi: X \mapsto \operatorname{Sig}(\widehat{X}) \tag{14}$$

is a universal feature map from the path space to the linear space of signatures [9]. To avoid computation over a large space of functions, we kernelize the signature feature map  $\Phi$  in Equation (14), and define the signature kernel  $k(\boldsymbol{a},\boldsymbol{b}) := \langle \Phi(\boldsymbol{a}), \Phi(\boldsymbol{b}) \rangle$ , for any discrete time series  $\boldsymbol{a}$  and  $\boldsymbol{b}$ , as suggested in [9]. Here  $\langle \cdot, \cdot \rangle$  is the inner product on the linear space of signatures.

Next, to measure the similarity between two discrete time series  $\boldsymbol{a}$  and  $\boldsymbol{b}$ , consider the distance induced by the signature kernel [28, 3, 14, 19, 9],

$$d_{\text{Sig}}(\boldsymbol{a}, \boldsymbol{b}) = k(\boldsymbol{a}, \boldsymbol{a}) - 2k(\boldsymbol{a}, \boldsymbol{b}) + k(\boldsymbol{b}, \boldsymbol{b}).$$
(15)

Small  $d_{\text{Sig}}(\boldsymbol{a}, \boldsymbol{b})$  implies a higher similarity between patterns in  $\boldsymbol{a}$  and  $\boldsymbol{b}$ , which suggests that  $\boldsymbol{a}$  and  $\boldsymbol{b}$  come from the same regime and share the similar seasonality. In practice, one may truncate the signature to depth N when computing Equation (15), and we denote the distance computed from the depth-N truncated signature by  $d_{\text{Sig},N}$ .

Finally, we adapt the weights in the two-step LASSO according to the signature kernel, this is called AdaWeight.Sig. It takes five hyper-parameters: a forecast horizon  $\Delta t$ , a window size  $l \in \mathbb{N}$ , a signature depth  $N \in \mathbb{N}^+$ , a temperature parameter  $\gamma \geq 0$ , and the distance metric  $d_{\text{Sig},N}$ .

More precisely, define  $\mathbf{z}_{\tau} := (\mathbf{z}_{\tau}, y_{\tau + \Delta t})$  for any  $\tau \in \mathbb{N}^+$ ; for any  $\tau_1, \tau_2 \in \mathbb{N}^+$  and  $\tau_1 < \tau_2$ , denote  $\mathbf{z}_{\tau_1:\tau_2} := (\mathbf{z}_{\tau_1}, \cdots, \mathbf{z}_{\tau_2})$  as a slice of the time series  $\{\mathbf{z}_t\}_{t \in \mathbb{N}^+}$  from time  $\tau_1$  to  $\tau_2$ . At each time t, AdaWeight.Sig takes the historical samples  $\{(\mathbf{z}_{\tau}, y_{\tau + \Delta t})\}_{1 \leq \tau \leq t - \Delta t}$  as input, and outputs an adaptive weight vector

$$\mathbf{W}^{(\Delta t)} := (w_1^{(\Delta t)}, w_2^{(\Delta t)}, \cdots, w_{t-\Delta t}^{(\Delta t)}) \in \mathbb{R}_{>0}^{t-\Delta t}, \tag{16}$$

with  $\sum_{\tau=1}^{t-\Delta t} w_{\tau}^{(\Delta t)} = 1$ . That is, AdaWeight.Sig will assign a higher weight  $w_{\tau}^{(\Delta t)}$  to the sample  $(\boldsymbol{x}_{\tau}, y_{\tau+\Delta t})$  if the seasonality pattern near time  $\tau$  is more similar to the current seasonality pattern embedded in the sample  $(\boldsymbol{x}_{t-\Delta t}, y_t)$ . Thus, when a new data sample arrives, the weight vector  $\boldsymbol{W}^{(\Delta t)}$  will be recomputed by the AdaWeight.Sig module, in order to adapt to changes in the recent data samples.

Adaptive two-step LASSO via signature kernel. Measuring similarity via signature kernel leads to a novel LASSO-based approach, in which we propose to adapt weights according to the similarities between time series data to capture seasonality and regime switching embedded in the data. In the case of forecasting models with signature transforms, comparing similarities of data translates to identifying "signature feature maps". This is the statistical equivalence of identifying different distributions for a given set of data, albeit in the linearized features space from the signature transform. Algorithm 2 summarizes this approach of adaptive two-step LASSO via signature kernel, by integrating AdaWeight.Sig outlined in Algorithm 1 with the LASSO approach.

# 4 Real-time performance

Our signature-based adaptive two-step LASSO algorithm has been implemented for the trucking operations in Amazon since November 2022. Performance analysis shows that our forecast model presents superior performance than commercially available forecast models, with prediction accuracy improvement by more than fivefold, and has an estimated annualized savings of \$50MM.

# Algorithm 1 Adaptive Weight via Signature Kernel (AdaWeight.Sig)

- 1: **Input**: forecast horizon  $\Delta t$ , window size l, signature depth N, temperature parameter  $\gamma$ , kernel-based distance metric  $d_{\text{Sig},N}$  (15), data set  $D = \{ \boldsymbol{z}_{\tau} = (\boldsymbol{x}_{\tau}, y_{\tau+\Delta t}) \}_{1 \leq \tau \leq t-\Delta t}$ .
- 2: **for**  $\tau = 1, 2, \dots, t \Delta t$  **do**
- 3: Compute the distance  $\delta_{\tau}$  between the truncated depth-N signatures of  $\mathbf{z}_{\tau-l:\tau}$  and  $\mathbf{z}_{t-\Delta t-l:t-\Delta t}$ :

$$\delta_{\tau} := d_{\operatorname{Sig},N} \left( \boldsymbol{z}_{\tau-l:\tau}, \boldsymbol{z}_{t-\Delta t-l:t-\Delta t} \right). \tag{17}$$

- 4: end for
- 5: **for**  $\tau = 1, 2, \dots, t \Delta t$  **do**
- 6: Compute the weight  $w_{\tau}$  according to

$$w_{\tau}^{(\Delta t)} := \frac{\exp(-\gamma \cdot \delta_{\tau})}{\sum_{\tau=1}^{t-\Delta t} \exp(-\gamma \cdot \delta_{\tau})}.$$
 (18)

- 7: end for
- 8: **Output**: the weight vector  $\boldsymbol{W}^{(\Delta t)} = (w_1^{(\Delta t)}, \cdots, w_{t-\Delta t}^{(\Delta t)})$ .

# Algorithm 2 Adaptive two-step LASSO with Signature Kernel

- 1: **Input**: regularization parameter  $\lambda$ , window size l, signature depth N, temperature parameter  $\gamma$ ,  $d_{\text{Sig},N}$  in Equation (15).
- 2: for  $\Delta t = 1, 2, \cdots, \Delta T$  do
- 3: Regime identification: Run AdaWeight.Sig (Algorithm 1) with  $\Delta t$ , l, N,  $\gamma$ ,  $d_{\text{Sig},N}$ , and  $D = \{(\boldsymbol{x}_{\tau}, y_{\tau+\Delta t})\}_{\tau=1,2,\cdots,t-\Delta t}$ . Output  $\boldsymbol{W}^{(\Delta t)}$  in (16).
- 4: **2-step LASSO**: Apply the 2-step LASSO method on the data set D, with  $\mathbf{W}^{(\Delta t)}$  and regularization parameter  $\lambda$ :

$$\widehat{\boldsymbol{\theta}}_{\text{LASSO},\Delta t}^{\lambda} \in \operatorname*{arg\,min}_{\boldsymbol{\theta} \in \mathbb{R}^d} \left\{ \sum_{\tau=1}^{t-\Delta t} w_{\tau}^{(\Delta t)} \cdot \left( y_{\tau+\Delta t} - \left[ \boldsymbol{x}_{\tau}, \operatorname{Sig}^{N}(y_{\tau-l:\tau}) \right] \cdot \boldsymbol{\theta} \right)^{2} + \lambda \|\boldsymbol{\theta}\|_{1} \right\}. \tag{19}$$

$$\overline{\boldsymbol{\theta}}_{\text{LASSO},\Delta t}^{\lambda} \in \underset{\text{supp}[\boldsymbol{\theta}] = \text{supp}[\widehat{\boldsymbol{\theta}}_{\text{LASSO},\Delta t}^{\lambda}]}{\text{arg min}} \left\{ \sum_{\tau=1}^{t-\Delta t} w_{\tau}^{(\Delta t)} \cdot \left( y_{\tau+\Delta t} - \left[ \boldsymbol{x}_{\tau}, \text{Sig}^{N}(y_{\tau-l:\tau}) \right] \cdot \boldsymbol{\theta} \right)^{2} \right\}.$$
(20)

5: Given  $x_t, y_t$ , make prediction on  $y_{t+\Delta t}$ :

$$\widehat{y}_{t+\Delta t} = \left[ \boldsymbol{x}_t, \operatorname{Sig}^N(y_{t-l:t}) \right] \cdot \overline{\boldsymbol{\theta}}_{LASSO, \Delta t}^{\lambda}.$$

- 6: end for
- 7: **Output:** the forecast  $(\widehat{y}_{t+1}, \cdots, \widehat{y}_{t+\Delta T})$ .

Table 1: Comparing national-level 3-month-ahead industry predictions with our model predictions

Month in 2021	Actual	Industrial prediction	% Error Ind. pre- diction	Our pre- diction	% Error Our pre- diction	% Accuracy improvement
$\overline{ ext{Apr}}$	\$2.44	\$1.89	23%	\$2.39	2%	1050 %
May	\$2.51	\$1.82	27%	\$2.45	2%	1250%
${f Jun}$	\$2.53	N/A	N/A	\$2.48	2%	N/A
$\mathbf{Jul}$	\$2.57	\$2.18	15%	\$2.53	2%	650%
$\mathbf{Aug}$	\$2.61	\$2.21	15%	\$2.58	1%	1400%
$\mathbf{Sep}$	\$2.71	\$2.23	18%	\$2.70	1%	1700%
Oct	\$2.72	\$2.36	13%	\$2.69	1%	1200%
Nov	\$2.72	\$2.38	13%	\$2.71	1%	1200%

Table 2: 12-week ahead model predictions across different regions.

• • •	N.A.	A	В	C	D	${f E}$
week ahead						
predic-						
tion						
1	1.06%	1.88%	1.53%	1.38%	1.26%	1.53%
2	1.53%	1.93%	2.76%	1.92%	2.08%	2.06%
3	1.55%	2.95%	2.18%	1.19%	2.21%	2.07%
4	1.61%	3.83%	1.87%	1.50%	2.67%	2.34%
5	1.33%	2.57%	2.73%	1.05%	2.99%	1.32%
6	1.44%	2.86%	2.96%	1.85%	2.78%	1.20%
7	1.64%	2.33%	5.69%	1.73%	2.77%	2.51%
8	1.86%	1.71%	5.25%	3.64%	2.55%	2.64%
9	1.88%	2.99%	4.86%	2.55%	3.69%	2.15%
10	2.30%	3.80%	3.31%	4.10%	2.13%	2.53%
11	2.60%	4.71%	5.54%	4.33%	2.06%	2.85%
<b>12</b>	2.38%	5.65%	5.25%	4.76%	2.74%	5.33%

Table 3: Comparison between predictions with and without adaptive signature kernel

Week	Actual	Prediction without signature kernel	% Error without signature kernel	Prediction with sig- nature kernel	% Error with signa- ture kernel
$\overline{10/31/21}$	3.37	3.30	2.31%	3.32	1.53%
11/7/21	3.45	3.27	5.19%	3.34	3.22%
11/14/21	3.46	3.25	5.88%	3.38	2.15%
11/21/21	3.52	3.22	8.65%	3.37	4.25%
11/28/21	3.48	3.16	9.28%	3.35	3.66%
12/5/21	3.49	3.15	9.85%	3.31	5.15%

Table 4: Our model predictions posted on June 25 2022

Region	Week	Actual	Prediction	% Error
N.A.	7/3/2022	1.95	1.93	1.34%
	7/10/2022	1.95	1.93	1.12%
	7/17/2022	1.94	1.95	0.37%
	7/24/2022	1.93	1.96	1.25%
	7/31/2022	1.94	1.95	0.90%
	7/3/2022	1.8	1.78	0.68%
	7/10/2022	1.8	1.76	2.06%
${f A}$	7/17/2022	1.76	1.76	0.04%
	7/24/2022	1.72	1.74	1.46%
	7/31/2022	1.66	1.73	4.03%
	7/3/2022	1.26	1.26	0.39%
	7/10/2022	1.21	1.27	4.68%
В	7/17/2022	1.21	1.25	3.44%
	7/24/2022	1.21	1.25	3.28%
	7/31/2022	1.24	1.25	1.25%
	7/3/2022	1.1	1.1	0.40%
	7/10/2022	1.08	1.09	0.70%
${f C}$	7/17/2022	1.02	1.08	5.32%
	7/24/2022	1.02	1.04	2.01%
	7/31/2022	1.02	1.01	0.60%
	7/3/2022	1.92	1.95	1.86%
	7/10/2022	1.94	1.96	0.99%
$\mathbf{D}$	7/17/2022	1.98	1.98	0.28%
	7/24/2022	2.01	2.03	1.06%
	7/31/2022	2.01	2.07	2.86%
${f E}$	7/3/2022	1.79	1.76	1.70%
	7/10/2022	1.76	1.75	0.75%
	7/17/2022	1.76	1.74	0.94%
	7/24/2022	1.76	1.73	1.89%
	7/31/2022	1.75	1.73	1.01%

Below we will present the real-time performance using data from April 2021 to July 2022. While this timeframe precedes the model's actual implementation due to confidentiality restrictions, it represents a particularly challenging period marked by both the COVID-19 pandemic and the Ukraine conflict, and allows us to demonstrate the model's effectiveness in volatile market conditions.

We will showcase the national-level prediction in North America (N.A.) along with five representative regions within North America, designated A, B, C, D, and E to protect proprietary information. We apply the relative error to measure model performances where

$$\text{relative error} \coloneqq \frac{|\text{actual rate} - \text{forecast rate}|}{|\text{actual rate}|}.$$

Predictions comparison between industry models and our model. We compare the performance of our model at the national-level predictions with the standard industry predictions for the April 2021 - November 2021 time period. Both our model predictions and industry predictions are made three months (twelve weeks) ahead of time, with monthly predictions obtained by aggregating weekly predictions. The detailed results are listed in Table 1.

In particular, our predictions (with a relative error of around 2%) are far superior to standard industry predictions (with a relative error of around 20%). The prediction accuracy is improved by more than fivefold.

Relative prediction errors up to twelve weeks. Table 2 reports the relative prediction error of our model for the national level and five regional predictions (A, B, C, D, and E), up to a twelve-week horizon. The prediction error moderately increases from around 1% for the one-week prediction to approximately 5% for the twelve-week prediction, remaining significantly lower than the industry standard of 15%.

Necessity of adaptive signature kernel. To demonstrate the necessity of the adaptive signature kernel, the key and novel component of our model, we compare the predictions from Algorithm 2 with and without the signature kernel in Equation (13). The results are reported in Table 3. The predictions presented here are for one representative region in North America on October 24, 2021. Evidently from Table 3, the errors without the signature kernel are larger (> 8%) even for short-term predictions. In contrast, the signature kernel method captures better the seasonality, and obtains a smaller relative error (< 5%) for short-term predictions. This table shows the effectiveness of incorporating the signature kernel in the forecast model.

**Short-term prediction error.** Table 4 reports the relative prediction error of our model for the national level and five regional predictions (A, B, C, D, and E), for a five-week horizon, with model predictions made on June 25, 2022. Most of the prediction errors are shown to be less than 2%.

### 5 Conclusion

This work presents a novel, highly accurate signature-based adaptive two-step LASSO forecasting model for transportation marketplace rates. Deployed at Amazon since November 2022, it delivers more than fivefold forecast accuracy improvements compared to industry models even amidst major market disruptions, with significant cost savings.

### References

- [1] Imanol Perez Arribas. 2018. Derivatives pricing using signature payoffs. arXiv preprint arXiv:1809.09466 (2018).
- [2] Alexandre Belloni and Victor Chernozhukov. 2013. Least squares after model selection in high-dimensional sparse models. *Bernoulli* 19, 2 (2013), 521–547.
- [3] Alain Berlinet and Christine Thomas-Agnan. 2011. Reproducing Kernel Hilbert Spaces in Probability and Statistics. Springer Science & Business Media.
- [4] Patric Bonnier, Patrick Kidger, Imanol Perez Arribas, Cristopher Salvi, and Terry Lyons. 2019. Deep signature transforms. In *Proceedings of the 33rd International Conference on Neural Information Processing Systems*. 3105–3115.
- [5] Kuo-Tsai Chen. 1954. Iterated Integrals and Exponential Homomorphism. *Proceedings of the London Mathematical Society* s3-4, 1 (1954), 502–512.
- [6] Kuo-Tsai Chen. 1957. Integration of Paths, Geometric Invariants and a Generalized Baker-Hausdorff Formula. *Annals of Mathematics* 65, 1 (1957), 163–178.
- [7] Didier Chételat, Johannes Lederer, and Joseph Salmon. 2017. Optimal two-step prediction in regression. *Electronic Journal of Statistics* 11, 1 (2017), 2519–2546.
- [8] Ilya Chevyrev and Terry Lyons. 2016. Characteristic functions of measures on geometric rough paths. Annals of Probability 44, 6 (2016), 4049–4082.
- [9] Ilya Chevyrev and Harald Oberhauser. 2022. Signature moments to characterize laws of stochastic processes. *Journal of Machine Learning Research* 23, 176 (2022), 1–42.
- [10] Junyoung Chung, Caglar Gulcehre, KyungHyun Cho, and Yoshua Bengio. 2014. Empirical evaluation of gated recurrent neural networks on sequence modeling. arXiv preprint arXiv:1412.3555 (2014).
- [11] Peter K Friz and Martin Hairer. 2020. A course on rough paths. Springer.
- [12] Peter K Friz and Nicolas B Victoir. 2010. Multidimensional stochastic processes as rough paths: theory and applications. Vol. 120. Cambridge University Press.
- [13] Everette S Gardner Jr. 2006. Exponential smoothing: The state of the art—Part II. *International journal of forecasting* 22, 4 (2006), 637–666.
- [14] Arthur Gretton, Karsten M Borgwardt, Malte J Rasch, Bernhard Schölkopf, and Alexander Smola. 2012. A kernel two-sample test. *Journal of Machine Learning Research* 13, 1 (2012), 723–773.
- [15] Ben Hambly and Terry Lyons. 2010. Uniqueness for the signature of a path of bounded variation and the reduced path group. *Annals of Mathematics* (2010), 109–167.
- [16] James D Hamilton. 1989. A new approach to the economic analysis of nonstationary time series and the business cycle. *Econometrica: Journal of the econometric society* (1989), 357–384.
- [17] Jasdeep Kalsi, Terry Lyons, and Imanol Perez Arribas. 2020. Optimal execution with rough path signatures. SIAM Journal on Financial Mathematics 11, 2 (2020), 470–493.

- [18] Patrick Kidger and Terry Lyons. 2020. Signatory: differentiable computations of the signature and logsignature transforms, on both CPU and GPU. In *International Conference on Learning Representations*.
- [19] Franz J Király and Harald Oberhauser. 2019. Kernels for sequentially ordered data. *Journal of Machine Learning Research* 20, 31 (2019), 1–45.
- [20] S Vasantha Kumar and Lelitha Vanajakshi. 2015. Short-term traffic flow prediction using seasonal ARIMA model with limited input data. European Transport Research Review 7, 3 (2015), 1–9.
- [21] Chenyang Li, Xin Zhang, and Lianwen Jin. 2017. LPSNet: a novel log path signature feature based hand gesture recognition framework. In *Proceedings of the IEEE International Conference on Computer Vision Workshops*. 631–639.
- [22] Terry Lyons, Sina Nejad, and Imanol Perez Arribas. 2019. Numerical method for model-free pricing of exotic derivatives in discrete time using rough path signatures. *Applied Mathematical Finance* 26, 6 (2019), 583–597.
- [23] Terry Lyons, Hao Ni, and Harald Oberhauser. 2014. A feature set for streams and an application to high-frequency financial tick data. In *Proceedings of the 2014 International Conference on Big Data Science and Computing*. 1–8.
- [24] Terry J Lyons, Michael Caruana, and Thierry Lévy. 2007. Differential equations driven by rough paths. Springer.
- [25] James Morrill, Adeline Fermanian, Patrick Kidger, and Terry Lyons. 2020. A generalised signature method for multivariate time series feature extraction. arXiv preprint arXiv:2006.00873 (2020).
- [26] Robert H Shumway, David S Stoffer, Robert H Shumway, and David S Stoffer. 2017. ARIMA models. *Time series analysis and its applications: with R examples* (2017), 75–163.
- [27] Carl-Johann Simon-Gabriel and Bernhard Schölkopf. 2018. Kernel distribution embeddings: Universal kernels, characteristic kernels and kernel metrics on distributions. *Journal of Machine Learning Research* 19, 1 (2018), 1708–1736.
- [28] Bharath K Sriperumbudur, Arthur Gretton, Kenji Fukumizu, Bernhard Schölkopf, and Gert RG Lanckriet. 2010. Hilbert space embeddings and metrics on probability measures. The Journal of Machine Learning Research 11 (2010), 1517–1561.
- [29] James W Taylor. 2004. Smooth transition exponential smoothing. *Journal of Forecasting* 23, 6 (2004), 385–404.
- [30] Robert Tibshirani. 1996. Regression shrinkage and selection via the lasso. *Journal of the Royal Statistical Society: Series B (Methodological)* 58, 1 (1996), 267–288.
- [31] Zecheng Xie, Zenghui Sun, Lianwen Jin, Hao Ni, and Terry Lyons. 2017. Learning spatial-semantic context with fully convolutional recurrent network for online handwritten chinese text recognition. *IEEE transactions on pattern analysis and machine intelligence* 40, 8 (2017), 1903–1917.
- [32] Weixin Yang, Lianwen Jin, and Manfei Liu. 2015. Chinese character-level writer identification using path signature feature, DropStroke and deep CNN. In 2015 13th International Conference on Document Analysis and Recognition (ICDAR). IEEE, 546–550.
- [33] Yong Yu, Xiaosheng Si, Changhua Hu, and Jianxun Zhang. 2019. A review of recurrent neural networks: LSTM cells and network architectures. *Neural computation* 31, 7 (2019), 1235–1270.

- [34] Peng Zhao and Bin Yu. 2006. On model selection consistency of Lasso. *The Journal of Machine Learning Research* 7 (2006), 2541–2563.
- [35] Hui Zou. 2006. The adaptive lasso and its oracle properties. *Journal of the American statistical association* 101, 476 (2006), 1418–1429.